

Evidence for an anti-structure-pair in GaAs generated by electron irradiation at room temperature obtained from optically detected electron-nuclear double resonance

K. Krambrock and J.-M. Spaeth

University of Paderborn, Fachbereich Physik, Warburger Strasse 100 A, D-4790 Paderborn, Germany

(Received 1 July 1992)

The microscopic structure of a paramagnetic arsenic antisite-related defect in GaAs electron irradiated at room temperature has been studied using optically detected electron-nuclear double resonance (ODENDOR). In addition to the ODENDOR lines of the nearest and next-nearest As ligands those of a Ga atom have been observed. The analysis of the Ga ODENDOR lines gives evidence to identify this As antisite-related defect with an anti-structure-pair $\text{As}_{\text{Ga}}\text{-Ga}_{\text{As}}$, where the Ga_{As} is diamagnetic and located in the next-nearest As shell of the As antisite.

Electron irradiation has been used to produce intrinsic point defects in semiconductors. Electron paramagnetic resonance (EPR) experiments have shown that As antisite-related defects can be produced by electron irradiation at room temperature (RT) in all types of GaAs.¹⁻⁴ Differences were observed in the introduction rate of the As antisite-related defects: in *n*-type GaAs it ranges from 1 to 10 cm^{-1} and in semi-insulating (SI) and *p*-type GaAs it is of the order of 10^{-2}cm^{-1} . However, from EPR experiments alone it is not possible to determine their precise microscopic structure because only the hyperfine (hf) interaction with the ⁷⁵As antisite atom ($I = \frac{3}{2}$ and 100% abundance) is resolved, resulting in the typical quartet fingerprint EPR spectrum known from the *EL2* defect. Superhyperfine (shf) interactions which would give detailed information on the microscopic structure are not resolved. It has become evident in recent years that the different As antisite-related defects always show nearly the same EPR spectrum. However, they can be clearly distinguished by their magnetic circular dichroism of the optical absorption (MCDA).^{5,6}

Recently we have identified the isolated As antisite defect using optically detected electron-nuclear double resonance (ODENDOR).⁷ This defect can be produced by electron irradiation at low temperatures in GaAs crystals which contain *EL2* defects before irradiation. The isolated As_{Ga} defect was found to be not stable at RT.

In this Brief Report we report on an ODENDOR investigation of the As antisite-related defect produced by electron irradiation at RT which was observed by us previously in MCDA and optically detected electron paramagnetic resonance (ODEPR) measurements and called $\text{As}_{\text{Ga}}\text{-X}_1$.⁶ From the analysis of the ODENDOR spectra, there is clear evidence to identify this defect with an anti-structure-pair where the Ga_{As} atom is diamagnetic and located in the second-nearest As shell of the As antisite. A possible mechanism for the formation of this defect is presented. To the best of our knowledge, this is the first identification of such a pair in GaAs on a microscopic level. The results will be compared to those of the *EL2* defect, which was previously shown using ODENDOR to be an As antisite-As interstitial (As_{Ga} -

As_i) pair defect.⁸

Different types of GaAs crystals were investigated: *n*-type doped either with Si or Te with concentrations of $4 \times 10^{17} \text{cm}^{-3}$, different undoped semi-insulating and *p*-type undoped Ga rich or doped with Zn. The electron irradiations were performed at Forschungszentrum Jülich G.m.b.H. with a van de Graaff accelerator at an energy of 2 MeV and a dose between 5×10^{16} and $5 \times 10^{17} \text{cm}^{-2}$ at 4.2 K, with the samples kept at 77 K prior to the measurements or at 300 K with cooling such that heating of the samples was avoided. The experimental setup for the magneto-optical and the ODEPR and the ODENDOR experiments is described elsewhere.⁹

After irradiation with a dose of $5 \times 10^{17} \text{cm}^{-2}$ one dominant MCDA spectrum was observed in all types of GaAs crystals (Fig. 1). In ODEPR, the characteristic quartet spectrum of an As antisite-related defect was measured. The hf splitting and the *g* factor are identical to those of both the *EL2* defect and the isolated As_{Ga} defect within experimental error. Only the half-width of the four ODEPR lines are within 40 mT broader than those of the isolated As_{Ga} (32 mT) and of the *EL2* defect (34 mT).⁷ A clear difference between the several As antisite species was found in the excitation spectra of the ODEPR [MCDA "tagged by EPR" (Ref. 9)]. The ODEPR excitation spectrum of this As antisite-related defect is identical to the whole MCDA as measured in Fig. 1 and is totally different from the corresponding spectra of the *EL2* and the isolated As_{Ga} defects.⁷ Therefore this defect must have yet another microscopic structure. It must be another As_{Ga} -related complex.

In the MCDA spectrum one observes a so-called zero-phonon line (ZPL) at 1.130 eV with replicas separated by 11 meV (see inset in Fig. 1).⁶ The replica structure is practically identical to that of the ZPL of the *EL2* defect in the diamagnetic charge state.¹⁰ In comparison to *EL2*, the ZPL observed here is shifted to higher energy by 90 meV, slightly split, and belongs to the paramagnetic charge state (+/+ +) at 0.67 eV above the valence band.⁶ The ODEPR excitation spectrum also reproduces the ZPL and the replica structure, which shows directly that they do belong to the paramagnetic charge state. An

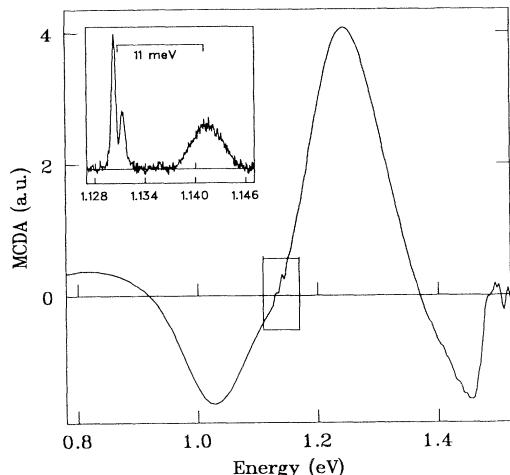


FIG. 1. MCDA spectrum of an As antisite-related defect ($\text{As}_{\text{Ga}}\text{-X}_1$) in *n*-type GaAs doped with Te (concentration: $4 \times 10^{17} \text{ cm}^{-3}$) after electron irradiation at RT (dose: $5 \times 10^{17} \text{ cm}^{-2}$) measured at 1.5 K and 2 T. Inset: so-called ZPL with first phonon replica measured in MCDA with higher spectral resolution (main MCDA line was subtracted).

interesting point is the small splitting of the ZPL of 0.9 meV without application of uniaxial stress. Such a splitting of the ZPL is not observed for the *EL2* defect. It indicates a stronger distortion in the nearest neighborhood in this antisite compared to that in the $\text{As}_{\text{Ga}}\text{-As}_i$ pair defect.

In the ODENDOR spectra, measured at 1.5 K, lines from the nearest ^{75}As ligands were found in the frequency range between 30 and 200 MHz. Two subshells with $\langle 111 \rangle$ symmetry could be identified, i.e., there are two different types of As ligands with different shf tensors which have both their principal axes (those with largest interaction) approximately in the $\langle 111 \rangle$ directions. Small deviations from axial symmetry could not be resolved. The shf interaction parameters are listed in Table I. We think that three neighbors are equivalent

TABLE I. Hyperfine and superhyperfine interaction parameters of the next-nearest $\text{As}_{\text{Ga}}\text{-Ga}_{\text{As}}$ anti-structure-pair: *a* isotropic hf or shf, *b* anisotropic hf or shf, and *q* quadrupole interaction constant. The interaction constants are related to the axial hf (shf) tensor \vec{A} by $A_{\parallel} = a + 2b$ and $A_{\perp} = a - b$ and to the axial quadrupole tensor \vec{Q} by $Q_{\parallel} = 2q$ and $Q_{\perp} = -q$. The tensor axis with the largest interaction is parallel to $\langle 111 \rangle$ in the first shell and parallel to the connection line ligand As_{Ga} for the second As shell sites. The precision of the shf and of the quadrupole interaction is ± 0.3 MHz.

	<i>a</i> / <i>h</i> (MHz)	<i>b</i> / <i>h</i> (MHz)	<i>q</i> / <i>h</i> (MHz)
Central $^{75}\text{As}_{\text{Ga}}$ nucleus	2600		
First ^{75}As shell: ligands 2–4:	205.4	50.8	11.1
Ligand 1:	158.5	54.7	12.9
Second ^{75}As shell:	23.5	2.4	0.5
^{69}Ga :	22.5	1.9	0.9
^{71}Ga :	28.6	2.4	0.6

and one is different, but cannot exclude that each subshell contains two ligands. There must be four nearest As ligands, otherwise the EPR linewidth cannot be explained, which excludes the model of an As_{Ga} with an As vacancy as a nearest neighbor.¹¹ The lower symmetry of the nearest neighborhood is clearly different from what we have found for the isolated As_{Ga} (Ref. 7) and also for the *EL2* defect,⁸ where the four nearest neighbors have almost identical shf interactions with $\langle 111 \rangle$ symmetry. There is a clear deviation from tetrahedral symmetry here, which also shows up in the splitting of the ZPL.

A new feature was observed in the frequency range between 10 and 35 MHz, where the second-shell As neighbors of both the isolated As_{Ga} and the *EL2* are measured [see Figs. 2(a) and 2(c)]. It is particularly in this shell that the lower symmetry of the *EL2* defect compared to the high symmetry of the isolated As_{Ga} becomes apparent by the observation of three subshells $\text{III}_{a,b,c}$.^{7,8} Apart from the second-shell As lines, there are additional lines due to the two Ga isotopes [Fig. 2(b)]. The assignment to Ga was made on the basis of the measurement of the magnetic-field dependence of the ODENDOR lines (Fig. 3). According to a first-order perturbation calculation of the appropriate spin Hamiltonian,¹² the positions of the ODENDOR lines shift linearly with the magnetic field *B*:

$$\nu_{\text{ENDOR}} = \frac{1}{2h} |A_{\text{shf}} m_s \pm g_n \mu_n B|, \quad (1)$$

where A_{shf} is the shf interaction parameter, g_n the nuclear *g* factor of the measured nucleus, and μ_n the nuclear magneton.¹² The result is shown in Fig. 3(b). Ga has two isotopes: ^{69}Ga with 60% abundance and ^{71}Ga

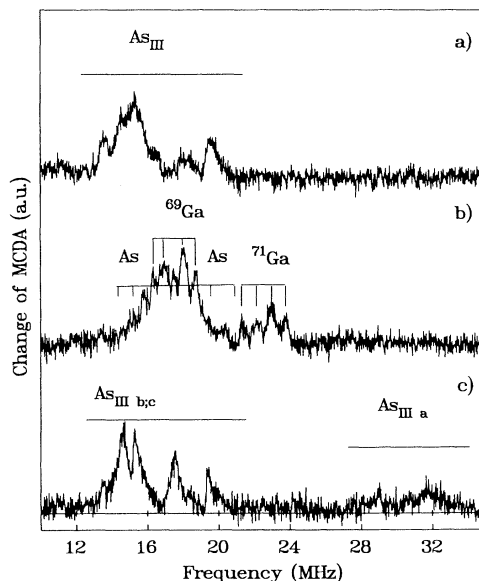


FIG. 2. ODENDOR spectra in the frequency range between 10 and 35 MHz of three different As antisite-related defects measured at 1.5 K for $B \parallel [001]$: (a) the isolated As_{Ga} defect (Ref. 7); (b) the $\text{As}_{\text{Ga}}\text{-X}_1$ defect; and (c) the *EL2* defect (Ref. 7). The ODENDOR lines from ^{75}As belong to the second As shells. In the case of the $\text{As}_{\text{Ga}}\text{-X}_1$ defect, additional ODENDOR lines from the two isotopes ^{69}Ga and ^{71}Ga were observed.

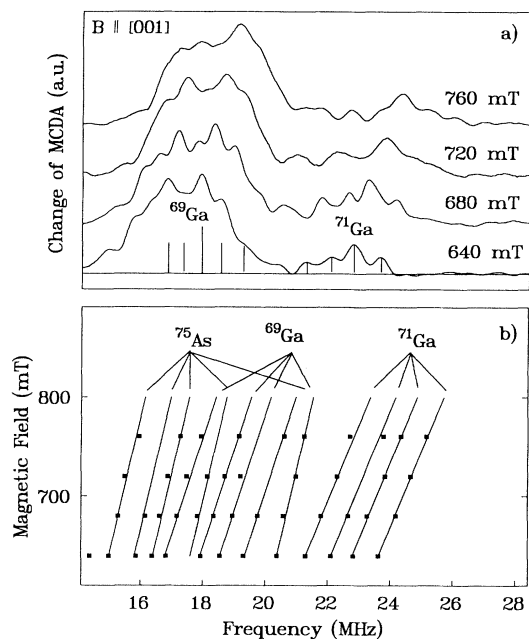


FIG. 3. (a) ODENDOR spectra of the $\text{As}_{\text{Ga}}\text{-X}_1$ defect in the frequency range between 14 and 28 MHz for $B \parallel [001]$ measured as a function of the magnetic field. (b) Squares mark the frequency positions of the peaks of the ODENDOR lines as a function of the magnetic field. The straight lines show the linear shift of the ODENDOR frequencies with the magnetic field, their slopes are proportional to the nuclear g factors of ^{75}As , ^{69}Ga , and ^{71}Ga , respectively.

with 40% abundance. Both the intensity ratios of the ODENDOR lines [Fig. 3(a)] and the magnetic-field shift of their frequencies [Fig. 3(b)] agree well with their assignment to the two Ga isotopes. Only ODENDOR lines of the $m_s = -\frac{1}{2}$ state appear in this frequency range.

The precise analysis of the angular dependence of these ODENDOR lines is very difficult because of the strong overlapping of lines. Figure 4 shows their angular dependence (squares) for rotation of the crystal in a $\{110\}$ plane. The lines cannot be due to a Ga interstitial in a $\langle 111 \rangle$ direction (analogous to the As_i in $\text{EL}2$). In this case, only three lines (if there is a quadrupole interaction) are expected for $B \parallel [001]$ since all nuclei would be equivalent. From the magnetic-field shift it is clear that at least four Ga lines are resolved for each isotope (Fig. 3). The analysis of the angular dependence agrees well with Ga interactions having a $\langle 110 \rangle$ symmetry as shown in Fig. 4(a) by the solid lines, which were calculated using the appropriate spin Hamiltonian containing shf and quadrupole interactions.¹² From the agreement with the experiment, it follows that one type of Ga ligand is either on a second-shell As site or on a site of the first Ga shell. Its shf axis (that with the largest interaction) is assumed to point to the As antisite (two shf axes are in a $\{110\}$ mirror plane of the defect containing the Ga and the As_{Ga}). The Ga neighbor has “ $\langle 110 \rangle$ symmetry.”¹³ There is only one Ga “shell,” i.e., only one Ga shf tensor for each isotope occurring in 12 $\langle 110 \rangle$ orientations. The interaction tensors were assumed to be axially symmetric.

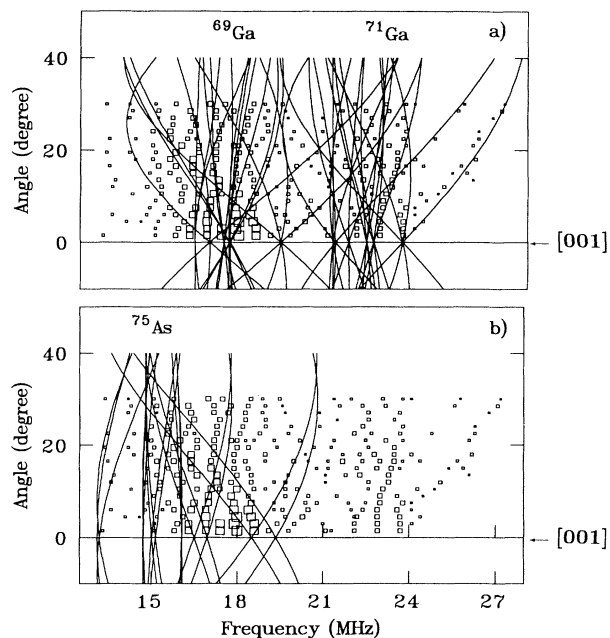


FIG. 4. Angular dependence of the ODENDOR lines of the $\text{As}_{\text{Ga}}\text{-X}_1$ defect in the frequency range between 10 and 28 MHz for a rotation of the magnetic field in a $\{110\}$ plane (0° corresponds to a $\langle 001 \rangle$ direction). The squares mark the frequency positions of the ODENDOR lines. (a) The solid lines are the calculated angular dependence for one Ga shell with $\langle 110 \rangle$ symmetry with the shf parameters of Table I. (b) The solid lines are the calculated angular dependence for the second-shell As ligands with $\langle 110 \rangle$ symmetry and the shf values of Table I (one shell was assumed, see text).

A more precise analysis detecting deviations from axial symmetry was not possible.

Neither in the isolated As_{Ga} (Ref. 7) nor in the $\text{EL}2$ defect⁸ have any Ga lines from the Ga shell been observed. Thus it seems not very reasonable to assign the Ga lines to the Ga shell. Furthermore, since the nearest As neighbors are clearly distorted from T_d symmetry, one would also expect that the Ga shell is broken into different subshells by the perturbation, which is the reason for the low nearest-neighbor symmetry. However, this would lead to many more Ga ODENDOR lines than we have observed. A Ga vacancy in this shell, which may cause the occurrence of spin density in the Ga shell, would also lower the symmetry to several Ga subshells. Because only one Ga interaction with $\langle 110 \rangle$ symmetry was measured, only one extra Ga atom can participate in this defect, except for the Ga ligands in the Ga shell which must have a vanishing or very small shf interaction. Its nearest location would be a next-nearest-neighbor (nnn) position in the second As shell. The resulting defect is the next nearest anti-structure-pair $\text{As}_{\text{Ga}}\text{-Ga}_{\text{As}}$ (nnn).

The angular dependence of the second As shell ($\langle 110 \rangle$ symmetry) could be explained similarly to that for the isolated As_{Ga} defect and the $\text{EL}2$ defect [Fig. 4(b), solid lines]. The shf interactions (Table I) are very similar to those found for the isolated As_{Ga} (Ref. 7) and to the shells $\text{III}_{b,c}$ of the $\text{EL}2$ defect, which are not influenced by the

As interstitial. We cannot say whether the second As shell is split into subshells with slightly different shf tensors. If there is a difference, it is much smaller compared to that between shell III_a and shells III_{b,c} of the *EL2* defect.⁸

In the GaAs crystals irradiated at low temperature, another defect is prominent in MCDA and ODEPR. On the basis of EPR experiments, this defect was recently attributed to the Ga vacancy in the (2-) charge state, trigonally distorted because of the Jahn-Teller relaxations.¹⁴ This defect is not very stable at RT and upon its decay the anti-structure-pair appears. We propose that near RT an As atom from the second-nearest As shell jumps into the Ga vacancy, forming an As_{Ga}-V_{As} (nnn) pair defect. Interstitial Ga, which is assumed to be mobile near RT,¹⁵ goes into the second-shell As vacancy, and the resulting defect is our anti-structure-pair consisting of an As antisite and a Ga antisite separated by 4.88 Å. So far, we have observed only the As_{Ga}⁺-Ga_{As} (nnn) charge state, where Ga_{As} (nnn) is diamagnetic. We assume Ga_{As} to be Ga_{As}²⁻, which would provide Coulomb attraction to As_{Ga}⁺. The unpaired spin density at Ga_{As} (nnn) is approximately 1%, the same as for the second-shell As. This is very different from As_i in the *EL2* defect, which carries 12% unpaired spin density, indicating a chemical bonding. In the anti-structure-pair there seems to be only a Coulomb attraction between the two partners.

Theoretical calculations for the thermal stability of this

pair do not exist. For the nearest As_{Ga}-Ga_{As} pair, calculations¹¹ show that this pair has one state with *E* symmetry in the band gap and is a simple donor with the (0/+) level at $E_{vb} + 0.3$ eV, where *vb* denotes the valence band. In the neutral charge state, the *E* state is occupied by four electrons and is diamagnetic. Since the Fermi level in our crystal is pinned at $E_{vb} + 0.67$ eV, we would not be able to see with magnetic resonance if the nearest anti-structure-pair is present. For the next nearest anti-structure-pair the energies are higher, since it has retained more of the As_{Ga} character.¹¹ The spin density which is 18% on the central As antisite atom is typical for an As antisitelike defect and the same as found for the isolated As_{Ga} and for the *EL2* defect.⁶

In conclusion, the analysis of the ODENDOR measurements of the As antisite-related defect produced by electron irradiation of RT gives clear evidence for an anti-structure-pair defect where the Ga_{As} is diamagnetic and located in the second As shell of the As antisite. Further details of the ODENDOR investigation, and in particular the optical properties of the As_{Ga}-Ga_{As} (nnn) in comparison to those of the isolated As_{Ga} and the *EL2* defect (in particular its metastability upon optical excitation), will be published elsewhere.

This work was supported by the BMFT "Erforschung kondensierter Materie und Atomphysik im Verbund mit Großgeräten" 3-Sp-2PAD-3.

¹N. K. Goswami, R. C. Newman, and J. E. Whitehouse, *Solid State Commun.* **40**, 473 (1981).

²T. A. Kennedy, B. J. Faraday, and N. D. Wilsey, *Bull. Am. Phys. Soc.* **26**, 255 (1981).

³R. B. Beall, R. C. Newman, J. E. Whitehouse, and J. Woodhead, *J. Phys. C* **18**, 3273 (1985).

⁴H. J. von Bardeleben, A. Miret, H. Lim, and J. C. Bourgoin, *J. Phys. C* **20**, 1353 (1987).

⁵J.-M. Spaeth, K. Krambrock, and D. M. Hofmann, in *The Physics of Semiconductors*, edited by E. M. Anastassakis and J. D. Joannopoulos (World Scientific, Singapore, 1990), Vol. 1, p. 441.

⁶J.-M. Spaeth, M. Fockele, and K. Krambrock, *Mater. Sci. Eng. B* **13**, 261 (1992).

⁷K. Krambrock, J.-M. Spaeth, C. Delerue, G. Allan, and M. Lannoo, *Phys. Rev. B* **45**, 1481 (1992).

⁸B. K. Meyer, D. M. Hofmann, J. R. Niklas, and J.-M. Spaeth, *Phys. Rev. B* **36**, 1332 (1987).

⁹J.-M. Spaeth, *Exp. Tech. Phys.* **36**, 257 (1988).

¹⁰M. Kaminska, *Rev. Phys. Appl.* **23**, 793 (1988).

¹¹G. A. Baraff and M. Schlüter, *Phys. Rev. B* **33**, 7346 (1986).

¹²H. Seidel, *Z. Phys.* **165**, 218 (1962).

¹³J.-M. Spaeth and F. K. Koschnik, *J. Phys. Chem. Solids* **52**, 1 (1991).

¹⁴Y. G. Jia, H. J. von Bardeleben, D. Stievenard, and C. Delerue, *Phys. Rev. B* **45**, 1685 (1992).

¹⁵C. Corbel, F. Pierre, K. Saarinen, P. Hautojärvi, and P. Moser, *Phys. Rev. B* **45**, 3386 (1992).